Chemistry–A European Journal
Full Paper
doi.org/10.1002/chem.202005332
Chemistry Europe
European Chemical Societies Publishing

Liposomes

# Carbohydrate-Derived Metal-Chelator-Triggered Lipids for Liposomal Drug Delivery

Thomas Holmstrøm,[a] Mette Galsgaard Malle,[a] Shunliang Wu,[a] Knud Jørgen Jensen,[a] Nikos S. Hatzakis,[a, b] and Christian Marcus Pedersen*[a]

**Abstract:** Liposomes are versatile three-dimensional, biomaterial-based frameworks that can spatially enclose a variety of organic and inorganic biomaterials for advanced targeted-delivery applications. Implementation of external-stimuli-controlled release of their cargo will significantly augment their wide application for liposomal drug delivery. This paper presents the synthesis of a carbohydrate-derived lipid, capable of changing its conformation depending on the presence of $Zn^{2+}$: an active state in the presence of $Zn^{2+}$ ions and back to an inactive state in the absence of $Zn^{2+}$ or when exposed to $Na_2EDTA$, a metal chelator with high affinity for $Zn^{2+}$ ions. This is the first report of a lipid triggered by the presence of a metal chelator. Total internal reflection fluorescence microscopy and a single-liposome study showed that it indeed was possible for the lipid to be incorporated into the bilayer of stable liposomes that remained leakage-free for the fluorescent cargo of the liposomes. On addition of EDTA to the liposomes, their fluorescent cargo could be released as a result of the membrane-incorporated lipids undergoing a conformational change.

## Introduction

Liposomes are spherical nanoparticles with an aqueous interior formed by the self-assembly of lipids in an aqueous medium.[1] They can serve as a three-dimensional frame on which one can assemble or confine a spectrum of molecules of diverse functionalities, ranging from small molecules to genetic material and even large enzymes, and create autonomous, integrated systems of nanoscopic dimensions.[2,3] The ability to encapsulate small molecules has made it possible to use liposomes as a drug-delivery platform. This can reduce the toxicity of the drug, enhance its lifetime, and improve its pharmacokinetic profile.[4] When drug-loaded liposomes circulate in the body, they are subjected to natural degradation by the metabolism.[2] As this promotes the release of the drug at locations where it is not effective, liposomes equipped with stimuli-responsive lipids for controlled release have been developed along with the development and implementation of stealth liposomes.[3,5,6] Over the last couple of years, a growing amount of research has dealt with the development of stimuli-responsive lipids that can change their amphiphilic properties on an external stimulus such as a change in pH,[7,8] the presence of certain enzymes, or other changes in its environment.[5,9] If these lipids are incorporated into liposomes, then a change in their amphiphilic properties may cause the lipid membrane of the liposome to break down, such that its interior is exposed and its cargo is released. This offers specificity-encoded liposomes for drug delivery that can be targeted for specific, relevant areas of action. To the best of our knowledge, there have not yet been reports of stimuli-responsive lipids triggered by the presence of metal chelators. We believe that biological metal chelators such as metallothioneins (MTs) may serve as a relevant area of action for these targeted, liposomal drug-delivery systems as, for example, increased expression of MTs in breast cancer, ovarian cancer, nasopharyngeal cancer, urinary bladder cancer, and melanoma has been observed.[10–14] A lipid with such a metal-chelator-responsive property must be designed around already known metal-ion-triggered lipids.

Recently Veremeeva et al.[15,16] presented the first metal-ion-triggered lipid, which was designed on the basis of a bispidinone scaffold, capable of performing a conformational change when complexing $Cu^{2+}$ ions. Incorporation of the lipid into liposomes that could then be triggered by $Cu^{2+}$ ions cleared the way for further design. Later, Lou et al.[17] presented a lipid switch triggered by $Ca^{2+}$ ions, a biologically important ion, functioning by the same hinge principle. In 2015, Takeuchi et al.[18] presented a lipid that was triggered by the removal of a metal ion under strongly acidic conditions. Their lipids consisted of a carbohydrate with two lipophilic tails capable of undergoing a hinge-like motion when complexing $Zn^{2+}$ ions, thereby forming an amphiphilic compound. Incorporation of the $Zn^{2+}$-complexing lipids into liposomes gave stimuli-responsive nanocarriers capable of releasing an encapsulated

[a] T. Holmstrøm, M. Galsgaard Malle, S. Wu, K. J. Jensen, N. S. Hatzakis, C. M. Pedersen
Department of Chemistry, University of Copenhagen
Universitetsparken 5, 2100 Copenhagen (Denmark)
E-mail: cmp@chem.ku.dk

[b] N. S. Hatzakis
Novo Nordisk Foundation Center for Protein Research
University of Copenhagen, (Denmark)

Supporting information and the ORCID identification number(s) for the author(s) of this article can be found under:
https://doi.org/10.1002/chem.202005332.

fluorescent dye on addition of strong acid (HCl). According to Takeuchi et al., protonation of the binding sites expelled the complexed $Zn^{2+}$ ions, and the resulting reverse hinge motion ruptured the membrane.

Herein we present the synthesis and characterization of a metal-chelator-triggered lipid based on a carbohydrate scaffold. We have previously presented a carbohydrate-derived conformational switch that can be activated in the presence of $Zn^{2+}$ ions.[19] This has led to the development of a new lipid switch that, on complexation of $Zn^{2+}$ ions by two chelating picolyl groups, can undergo a ring flip from a $^4C_1$ to a $^1C_4$ conformation in a hinge-like motion to become an "active lipid", by the same principle previously applied by Veremeeva, Lou, and Takeuchi. The concept of the lipid is presented in Scheme 1.

During the ring flip of the pyranoside ring, two lipophilic tails are brought together in close proximity to form a compound with amphiphilic properties (Scheme 1 a), which is its active state. The bound metal ion can then be excluded from the carbohydrate lipid by the addition of a competing ligand, whereby the lipid returns to its inactive $^4C_1$ conformation (Scheme 1 b). We hypothesized that these lipids could be incorporated into liposomes while encapsulating a cargo (Scheme 1 c) and that this cargo could be released by the presence of a competing metal chelator, for example, MTs, as a result of the lipid bilayer being ruptured upon the conformational change performed by the lipid (Scheme 1 d).

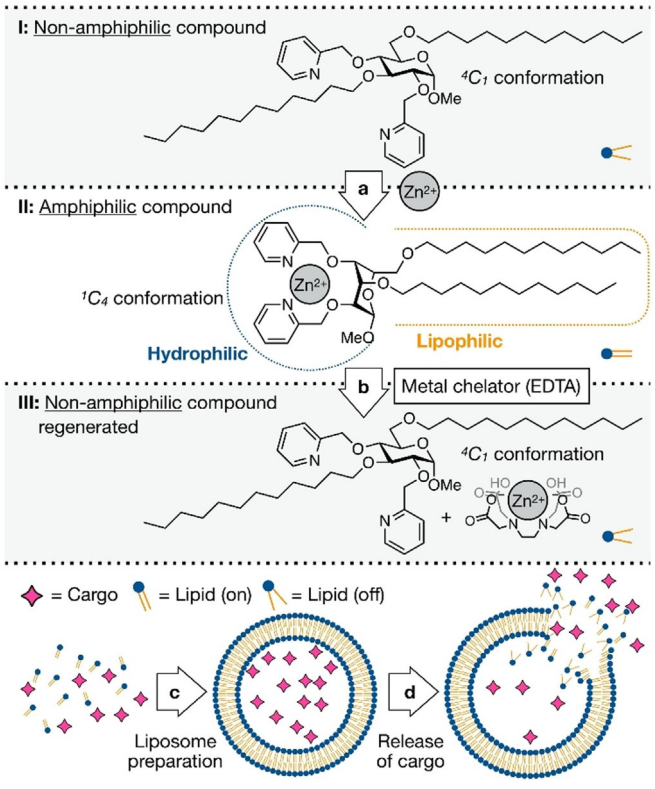


**Scheme 1.** Schematic representation of the carbohydrate-based, stimuli-responsive lipids: In its off (inactive) state, the pyranose ring exists in a $^4C_1$ conformation separating the two lipophilic C12 chains (I). On addition of $Zn^{2+}$ ions (a), a ring flip occurs rendering the two lipophilic chains in close proximity when the pyranose ring adopts a $^1C_4$ conformation (II). In this state the lipid becomes amphiphilic and it can self-assemble to form liposomes. In the presence of a competing metal chelator (b), the lipid converts back to its original $^4C_1$ conformation, rendering it non-amphiphilic (III). Cargo-loaded liposomes can be prepared from the lipids in the active (on) state (c). By removing $Zn^{2+}$ with, for example, EDTA, the cargo in the liposomes can be released (d).

## Results and Discussion

### Synthesis

As observed by Takeuchi et al.,[18] the length of the lipophilic chains in systems such as this has a great impact on the types of aggregates they form. We therefore decided to synthesize three different carbohydrate lipids with different chain lengths. Two of the three compounds were synthesized from a common intermediate **4** by a Williamson ether synthesis with different alkyl halides to afford the $C_{12}$ lipid **1** and the $C_6$ lipid **2** (Scheme 2).

The common intermediate **4** was synthesized in five steps from the readily available building block methyl α-D-glucopyranoside **9** by first protecting its four hydroxyl groups as trimethylsilyl (TMS) ethers. The TMS-protected pyranoside **8** was then regioselectively protected by using a procedure by Français et al. to afford the benzylidated pyranoside **7** without the need for chromatography.[20] Regioselective opening of the

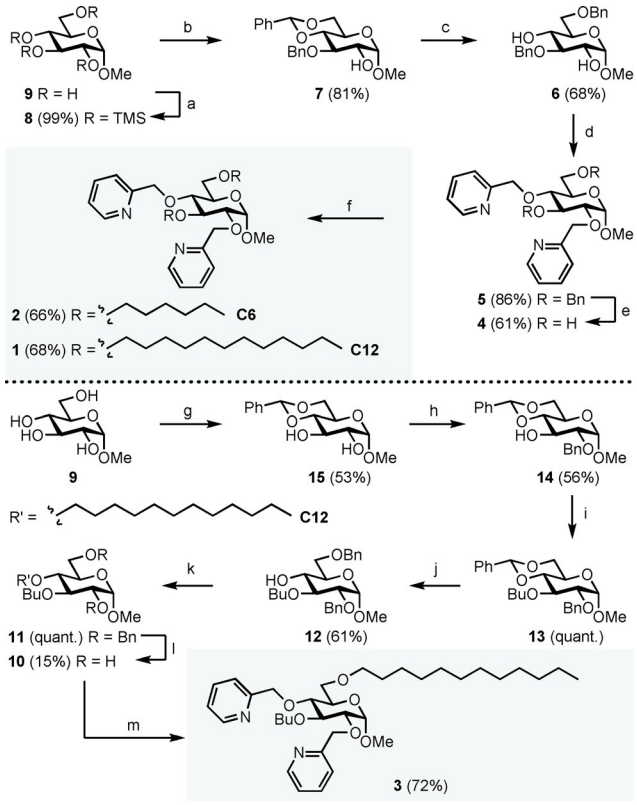


**Scheme 2.** Synthesis of the lipids. a) TMSCl, pyridine. b) PhCHO, TMSOTf, $Et_3SiH$, $CH_2Cl_2$. c) TFA, $Et_3SiH$, $CH_2Cl_2$. d) Picolyl chloride, NaH, tetra-*n*-butylammonium iodide, DMF. e) Pd/C, $NH_4HCO_3$, MeOH. f) 1-Bromohexane/1-bromododecane, NaH, DMF. g) Benzaldehyde dimethyl acetal, 10-CSA, MeCN. h) $Bu_2SnO$, MeOH, BnBr. i) BuBr, NaH, DMF. j) $BH_3$·THF, $Cu(OTf)_2$, THF. k) 1-Bromododecane, NaH, DMF. l) $H_2$, Pd/C, MeOH. m) Picolyl chloride, NaH, DMF.

benzylidene was carried out with triethylsilane in the presence of trifluoroacetic acid (TFA) to give 3,6-*O*-benzylated pyranoside **6**, which could then be functionalized with picolyl groups on the free 2- and 4-positions to give **5**. Finally, the two benzyl groups were removed with ammonium formate in the presence of Pd/C to give rise to the common intermediate **4**, alkylation of which gave lipids **1** and **2**. The third lipid **3** was functionalized with two different alkyl chains (dodecyl and butyl) and was therefore synthesized by the alternative route presented at the bottom of Scheme 2. The key intermediate **14** was synthesized from the same starting material **9** in two steps. First by installing a benzylidene protective group followed by regioselective benzylation with a dibutyltin acetal to afford methyl 2-*O*-benzyl-4,6-*O*-benzylidene α-D-glucopyranoside **14**. From here the remaining 3-OH group could be alkylated with 1-bromobutane, followed by regioselective opening of the benzylidene with $BH_3$·THF and $Cu(OTf)_2$ to afford the 6-*O*-benzylated pyranoside **12**. The 4-OH group was then alkylated with 1-bromododecane before it was subjected to debenzylation to give compound **10**. Finally the third lipid **3** was obtained by instalment of picolyl groups using picolyl chloride and NaH.

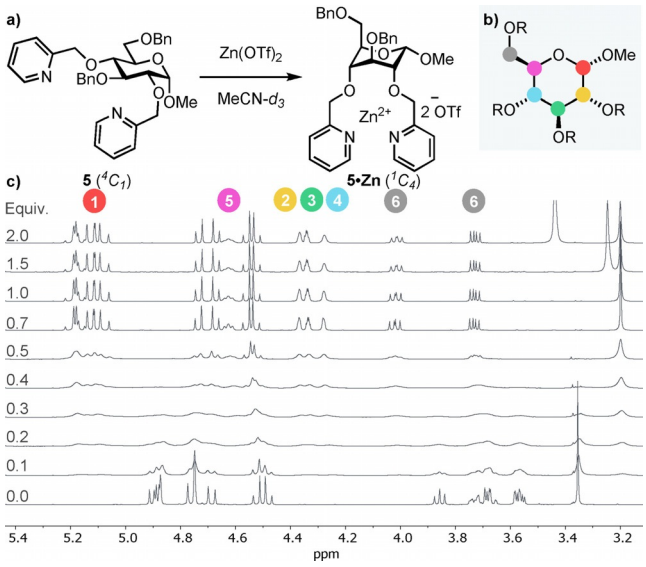


**Figure 1.** Titration of **5** with $Zn(OTf)_2$ in [$D_3$]acetonitrile. a) Conformations of **5** before and after the addition of the metal ions predicted by $^1$H NMR spectroscopy. b) Numbering of a pyranoside ring. c) $^1$H NMR spectra of **5** at different concentrations of $Zn^{2+}$.

## Metal binding properties

With the three lipids in hand, their ability to complex $Zn^{2+}$ ions was investigated by $^1$H NMR spectroscopy. By titrating samples of the lipids dissolved in [$D_3$]acetonitrile with $Zn(OTf)_2$ and recording a spectrum at fixed intervals, the binding behavior could be evaluated. Furthermore, information about the conformation of the pyranoside ring could be extracted from the vicinal coupling constants measured in the $^1$H NMR spectra. The $^1$H NMR spectra of all compounds underwent significant changes on addition of $Zn^{2+}$; however, due to broadening of the signals, it was only possible to assign a conformation to **3·Zn** and **5·Zn**. The $^1$H NMR spectrum of compound **5** gave the clearest information on its conformation due to only a few signals overlapping. From the $^1$H NMR titration of **5** with $Zn(OTf)_2$ (Figure 1), it can be seen that, on addition of between 0.1 and 0.7 equiv of $Zn^{2+}$ ions, broadening was observed, indicative of a medium-fast exchange between conformers. Sharpening of the spectrum already at 0.7 equiv of $Zn^{2+}$ ions could be due to the temporary formation of a 2:1 complex comprising two carbohydrates and one $Zn^{2+}$ ion, as we have earlier observed.[19] However, a UV/Vis titration of **5** with $Zn(OTf)_2$ revealed that 1.0 equiv of $Zn^{2+}$ ions were needed to completely saturate all binding sites, which indicates the presence of a 1:1 complex (see Supporting information, Figure S5). At 1.0 equiv of added $Zn(OTf)_2$, sharp signals corresponding to the desired **5·Zn** complex appeared in the $^1$H NMR spectrum, and the newly formed complex showed stability even on the addition of an excess amount of metal ions (Figure 1c). By analyzing the vicinal coupling constants (Table S1, Supporting Information), which were most pronounced for the signals arising from H2, H3, and H4, it became apparent that the pyranoside ring of compound **5** had taken on a $^1C_4$ conformation, the presumed conformation of the lipids in the active state (Scheme 1). Performing the same analysis on the spectrum of compound **5** before the addition of $Zn^{2+}$ confirmed a $^4C_1$ conformation, the inactive conformation. The same two conformations could be assigned to lipid **3** and **3·Zn** (see Supporting information, Figure S3).

Having established that the compounds are able to complex $Zn^{2+}$ ions and undergo a conformational change, we turned our attention to reversing the reaction, that is, going from a $^1C_4$ back to a $^4C_1$ conformation. This was attempted by the addition of a competing ligand with a stronger affinity for $Zn^{2+}$ ions than the pyridine groups of the lipids. Ethylenediaminetetraacetic acid disodium salt ($Na_2EDTA$) was an obvious choice of ligand due to its high affinity towards $Zn^{2+}$ ions ($K_{Zn} \approx 10^{16}$ M$^{-1}$). However, due to low solubility in acetonitrile, we found that tris[2-(dimethylamino)ethyl]amine ($Me_6TREN$) could be used as an alternative chelator.

The binding between $Me_6TREN$ and $Zn^{2+}$ is weaker than that of EDTA and $Zn^{2+}$ ($K_{Zn} = 5.6 \times 10^9$ M$^{-1}$ for $Me_6TREN$), but sufficient for this experiment.[21] To a solution of lipid **1** in [$D_3$]acetonitrile (Figure 2a) was added 1.0 equiv of $Zn(OTf)_2$ to generate **1·Zn** in situ (Figure 2b). On addition of 1.0 equiv $Me_6TREN$, new signals from the protons of the added ligand occurred in the $^1$H NMR spectrum. Furthermore, the broad signals arising from lipid **1·Zn** disappeared, and instead the signals of lipid **1** reappeared (Figure 2c), confirming the switching properties of lipid **1**.

## Aggregation properties

Knowing that all of the carbohydrate lipids could complex $Zn^{2+}$ ions and with the indication that the lipids were able to undergo a conformational change upon switching, we investigated their ability to self-assemble in an aqueous medium. First, the carbohydrate lipids were subjected to a preliminary dynamic light scattering (DLS) study in Milli-Q water at differ-

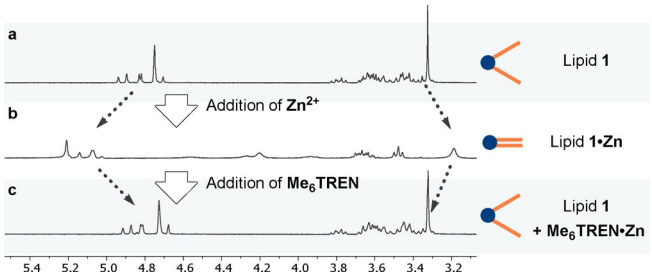


**Figure 2.** Evaluation of the back-reaction from **1·Zn** to **1** on addition of $Me_6$TREN: a) $^1$H NMR spectrum of **1** in [$D_3$]acetonitrile. b) $^1$H NMR spectrum of **1** in the presence of $Zn^{2+}$ ions. **1·Zn** was generated in situ. c) $^1$H NMR spectrum after addition of $Me_6$TREN to the same sample.

ent concentrations. It was found that all three carbohydrate lipids were able to form aggregates in water with low dispersity (see Supporting information, Figures S6–S8). The $C_{12}$ lipid **1·Zn** was even able to form monodisperse aggregates down to a concentration of 40 μM (43 mg $L^{-1}$); however, at a lower concentration (4 μM), the dispersity of the aggregates increased, that is, this concentration was below the critical aggregation concentration (CAC). This allowed us to determine the CAC of the three carbohydrate lipids using the convenient Nile Red method.[22] The CAC values are listed in Table 1. All lipids have CACs below 100 μM, and the $C_{12}$ lipid **1·Zn** has the lowest CAC of 35 μM (38 mg $L^{-1}$). This fit very well with the observation made in the preliminary DLS study on the same lipid. As a trend, it seemed that the CAC increased when shorter alkyl chains were introduced.

Due to the three carbohydrate lipids having almost similar aggregation properties, we chose to proceed with cargo-release studies using only the $C_{12}$ lipid **1·Zn**, as this had the lowest CAC among the three synthesized lipids.

**Table 1.** Critical aggregation concentration (CAC) and DLS data of the three carbohydrate lipids **1·Zn**, **2·Zn**, and **3·Zn**.

| Lipid | CAC | Hydrodynamic diameter [nm] | Polydispersity [%] |
|---|---|---|---|
| **1·Zn** | 35 μM (38 mg/L) | 412.5 ± 85.62 | 20 |
| **2·Zn** | 95 μM (89 mg/L) | 327.4 ± 58.25 | 17 |
| **3·Zn** | 50 μM (48 mg/L) | 312.6 ± 64.50 | 23 |

### Direct real-time observation of cargo release via EDTA

The cargo-release properties of lipid **1·Zn** were evaluated with a total internal reflection fluorescence (TIRF) microscopy setup. This setup can not only be used for the visualization of liposomes, but also for monitoring the release of an encapsulated fluorescent dye from intact liposomes. The general idea behind this assay is illustrated in Figure 3a: $Zn^{2+}$ removal would promote the transient formation of one or more pores, from which fluorescently labeled cargo would be released out of the liposomes.

Hundreds of liposomes per field of view were tethered on poly(L-lysine)-poly(ethylene glycol) (PLL-PEG)-passivated and PLL-PEG biotin-passivated surfaces.[23,24] This methodology maintains the spherical shape and structural integrity of the liposomes.[25] In the membrane of the liposomes were integrated ATTO488 DOPE and encapsulated in their lumen ATTO655 Carboxy chromophores. Real-time imaging of two microscope channels (one for each dye) allowed synchronous recording of both the cargo and the liposome membrane.[25] Three different types of liposomes were prepared in a phosphate-buffered saline (PBS): one active liposome containing lipid **1·Zn** and two control liposomes. The compositions of the three types of liposomes are listed in Table 2. All liposomes were composed of DOPC, DOPG, and DSPE-PEG(2000) biotin. The charged DOPG lipids were incorporated because they have been shown to render the liposomes unilamellar upon ten cycles of flash-freezing and thawing while the biotin-conjugated lipids made surface-immobilization possible, as is illustrated in Figure 3a.

After tethering of the liposomes to the surfaces, a flow of PBS buffer was used to wash away nonencapsulated dye and make visualization possible. Figure 3b shows a typical TIRF image in which hundreds of individual tethered liposomes are observed. The two-color imaging (see blue and red color zoom) shows the presence of liposomes in both channels (Figure 3b), which confirms that ATTO655 Carboxy was successfully encapsulated into the **1·Zn**-containing liposomes. Using a fluidic pump, we exposed the liposomes to a constant flow of a 10 mM solution of $Na_2$EDTA in PBS halfway through the experiment and throughout the remaining time of the experiment. $Na_2$EDTA was used in this case due to its high water solubility and high affinity to metal ions. Immediately after introducing $Na_2$EDTA to the liposomes, the ATTO655 chromophore escaped, as shown qualitatively for a few liposomes in the inset of Figure 3b and in the typical data for individual liposomes in Figure 3c, (see Supporting information, Figure S12 for additional traces). Notably, the intensity of the membrane-incorporated dye remained at a constant level (Figure 3b and c), that is, the cargo was released while liposomes remained bound and maintained their structural integrity. These data confirm the hypothesis of $Zn^{2+}$-dependent pore formation and cargo release of liposomes.

Several control experiments were performed to verify that the observed release was not an imaging artifact and to better understand the mechanism of the EDTA-promoted release. The liposome only containing DOPC was unaffected by the same addition of $Na_2$EDTA, and this suggests that lipid **1·Zn** is critical for the responsiveness of the lipids (Figure 3d, see Supporting information, Figure S13 for additional traces). We also prepared liposomes containing 50% in molar ratio of the inactive lipid **1**. Again, no release of fluorescent cargo was observed (Figure 3e, see Supporting information, Figure S14 for additional traces), and this further supports that lipid **1** is only active when binding $Zn^{2+}$ ions. Before being immobilized for TIRF microscopy, the liposomes were analyzed by DLS to evaluate their hydrodynamic diameter and polydispersity. Interestingly, both the DLS measurements and the TIRF data showed that the liposomes incorporated with **1·Zn** lipids and the reference

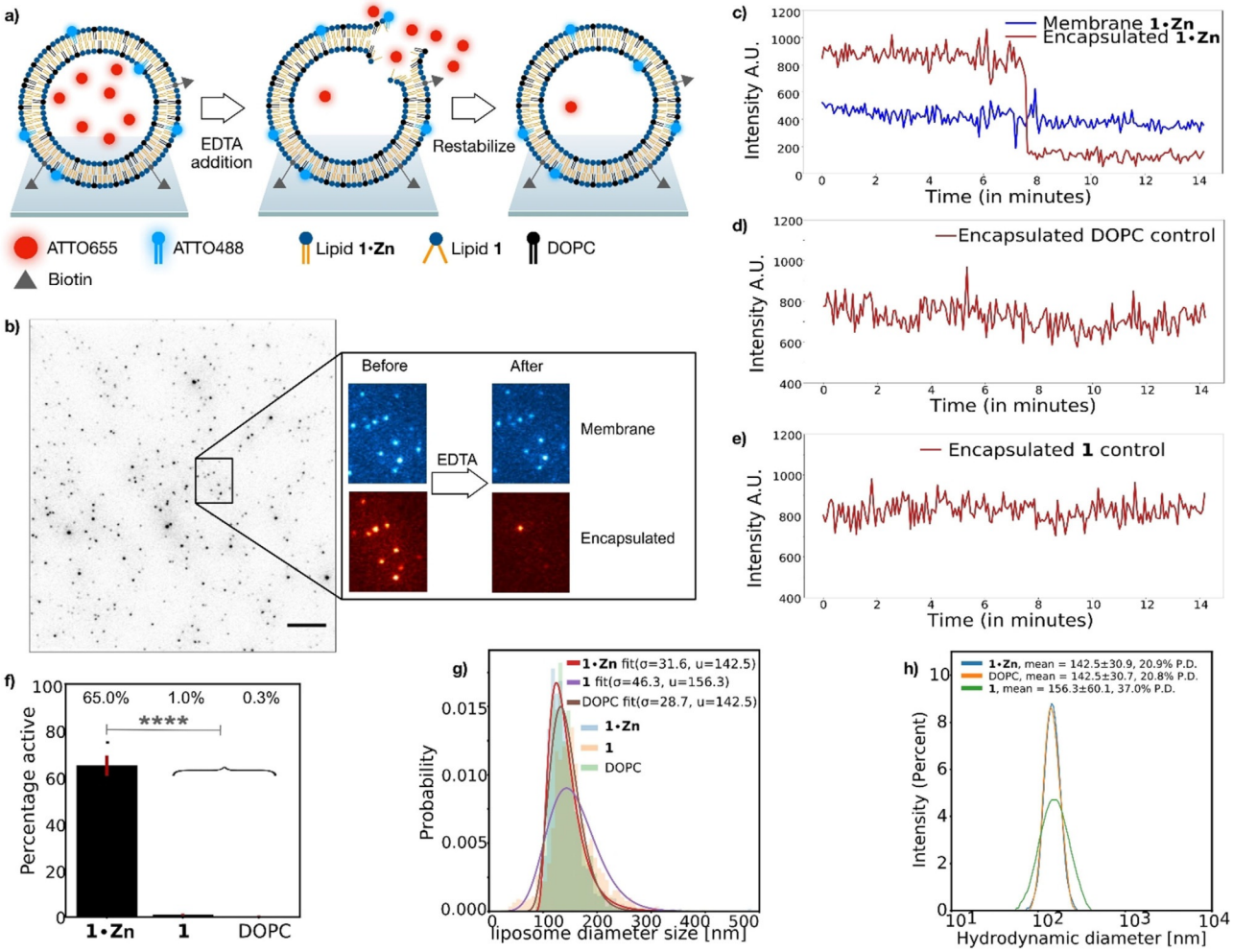


**Figure 3.** Cargo-release properties of lipid **1·Zn**. a) Illustration of the liposomes immobilized on a surface for TIRF microscopy. The liposomes contain **1·Zn** and ATTO488 (blue) in the membrane while encapsulating ATTO655 Carboxy (red). b) TIRF image of the immobilized liposomes (scale bar = 10 μm). The enlarged region shows the two emission channels before and after addition of $Na_2EDTA$, showing the release of the cargo (reduction in red), while liposomes remain bound and structurally intact (constant blue). c) Representative trajectory of an individual liposome containing **1·Zn** over time showing the release of cargo (red trace) simultaneous with a stable and preserved membrane (blue). d) Representative trajectory of liposomes containing DOPC over time showing no cargo release. e) Representative trajectory of liposomes containing **1** over time showing no cargo release. f) Percentage activity for all three liposome populations. Indicated $p$ value $< 0.0001$ % reveals a significant difference based on a two-sample t-test. g) Size distributions of the liposomes based on the encapsulated intensity and the DLS measurements. h) DLS data from all three liposomes. Error bars are one standard deviation.

**Table 2.** Composition of the prepared liposomes.

| Liposome | Lipid composition [mol %][a] |
|---|---|
| **1·Zn** | 50 % lipid 1·Zn, 48 % DOPC, 0.5 % ATTO488 DOPE, 1.5 % utility lipids |
| DOPC | 98.5 % DOPC, 1.5 % utility lipids |
| **1** | 50 % lipid 1, 48.5 % DOPC, 1.5 % utility lipids |

[a] Utility lipids: 1 % DOPG, 0.5 % DSPE-PEG(2000) biotin.

liposomes made purely with DOPC lipids were overlayed in size (Figure 3h) and in amount of encapsulated cargo (see Supporting information, Figure S15). The inactive lipid **1**, on the other hand, forms slightly more heterogenic liposomes in size and with a broadening in encapsulation of the dye, that is, the absence of $Zn^{2+}$ ions causes destabilization of the liposomes and the inactive lipid **1** in general is less willing to be incorporated into a lipid bilayer compared with lipid **1·Zn** or DOPC. However, as it was still possible to form liposomes with the inactive lipid **1**, the product of $Na_2EDTA$ addition, the active liposomes could possibly restabilize after releasing their cargo, forming liposomes or other aggregates still containing lipid **1** and the membrane-bound ATTO488 dye (Figure 3a).

The parallel readout and analysis of hundreds (> 700) of individual liposomes on six surfaces before and after $Na_2EDTA$ addition allowed us to quantify the fraction of **1·Zn** liposomes the responded to $Zn^{2+}$ removal.[23,25,26] It was found that 65.0 ± 4.4 % of the liposomes were active and responded to $Na_2EDTA$ (Figure 3g). The presence of liposomes not releasing the cargo may be attributed to potential heterogeneities in lipid composition or the formation of pores that are too small,[27] and could be investigated in future work with higher temporal resolution than the 3.6 s used for this investigation. By comparing the sizes of all **1·Zn** liposomes ($N = 1163$) and the subpopula-

tion of all active liposomes ($N = 755$) (see Supporting information, Figure S16), it was found that the activity of the liposomes and thereby pore formation was not size-dependent. This further demonstrates the rigidity of lipid **1**, as it can remain active in liposomes of different sizes. Performing the same analysis on the two control experiments revealed a practically zero activity percentage (1.0 and 0.3% respectively with $p < 0.0001$% based on a two-sampled t-test), showing a significant difference between the active and the two inactive control liposomes and supporting the $Zn^{2+}$ mediated release for **1**.

The cargo-release study revealed that an encapsulated dye could be released by exposing the immobilized liposomes to a solution of $Na_2EDTA$. We believe that EDTA is able to complex the limited amount of $Zn^{2+}$ bound to the membrane-incorporated lipid **1**. As indicated by the $^1H$ NMR binding study, removal of the $Zn^{2+}$ ions resulted in a reverse hinge motion of the two lipid tails, causing the lipid bilayer to temporary break apart and form pores, with release of the encapsulated dye followed by a restabilization step forming aggregates containing lipid **1**.

## Conclusion

We have synthesized a series of new carbohydrate-derived lipids that in the presence of $Zn^{2+}$ ions can alter their amphiphilic properties and potentially become a part of a liposomal drug-delivery system. Their metal-binding properties were evaluated by $^1H$ NMR spectroscopy to determine the conformation before and after the addition of metal ions. Interestingly, it was possible to force the lipids through the reverse conformational change on addition of a competing chelator such as $Me_6TREN$ or $Na_2EDTA$. When incorporated into liposomes, the switching behavior of **1·Zn** made it possible to promote the rapid release of an encapsulated ATTO655 Carboxy dye on exposure to $Na_2EDTA$. We believe that this stimuli-responsive lipid in the future may be applied in a liposomal drug delivery system targeting metal-chelating metallothionein proteins along with other proteins.

## *Acknowledgements*

T.H. acknowledges the Villum Foundation (grant 00022899) for financial support. N.S.H. acknowledges funding from Villum Foundation center of Excellence BIONEC (grant 18333) and Novo Nordisk foundation Center for Biopharmaceuticals and Biobarriers in Drug Delivery (Grand Challenge Program, grant number NNF16OC0021948) NSH is an associate member of the Novo Nordisk Foundation Center for Protein Research, which is supported financially by the Novo Nordisk Foundation (NNF14CC0001) We also thank Karen Martinez and Nikolaj Brinkenfeldt for providing us and helping us with the microplate reader used for CAC determination.

## Conflict of interest

The authors declare no conflict of interest.

**Keywords:** carbohydrates · drug delivery · lipids · liposomes · zinc

[1] A. Sorrenti, O. Illa, R. M. Ortuño, *Chem. Soc. Rev.* **2013**, *42*, 8200 – 8219.
[2] B. S. Pattni, V. V. Chupin, V. P. Torchilin, *Chem. Rev.* **2015**, *115*, 10938 – 10966.
[3] V. P. Torchilin, *Nat. Rev. Drug Discovery* **2005**, *4*, 145 – 160.
[4] F. Perche, V. P. Torchilin, *J. Drug Delivery.* **2013**, *2013*, 705265.
[5] J. Lou, X. Zhang, M. D. Best, *Chem. Eur. J.* **2019**, *25*, 20 – 25.
[6] M. L. Immordino, F. Dosio, L. Cattel, *Int. J. Nanomed.* **2006**, *1*, 297 – 315.
[7] Y. Zheng, X. Liu, N. M. Samoshina, V. V. Samoshin, A. H. Franz, X. Guo, *Biochim. Biophys. Acta Biomembr.* **2015**, *1848*, 3113 – 3125.
[8] Y. Zheng, X. Liu, N. M. Samoshina, V. V. Samoshin, A. H. Franz, X. Guo, *Chem. Phys. Lipids* **2018**, *210*, 129 – 141.
[9] J. Lou, M. D. Best, *Chem. Eur. J.* **2020**, *26*, 8597 – 8607.
[10] M. G. Cherian, A. Jayasurya, B.-H. Bay, *Mutat. Res. Mol. Mech. Mutagen.* **2003**, *533*, 201 – 209.
[11] M. Si, J. Lang, *J. Hematol. Oncol.* **2018**, *11*, 107.
[12] P. Coyle, J. C. Philcox, L. C. Carey, A. M. Rofe, *Cell. Mol. Life Sci. C* **2002**, *59*, 627 – 647.
[13] M. Margoshes, B. L. Vallee, *J. Am. Chem. Soc.* **1957**, *79*, 4813 – 4814.
[14] C. Jacob, W. Maret, B. L. Vallee, *Proc. Natl. Acad. Sci. USA* **1998**, *95*, 3489 – 3494.
[15] P. N. Veremeeva, V. L. Lapteva, V. A. Palyulin, D. A. Davydov, A. A. Yaroslavov, N. S. Zefirov, *Dokl. Chem.* **2012**, *447*, 275 – 277.
[16] P. N. Veremeeva, V. L. Lapteva, V. A. Palyulin, A. V. Sybachin, A. A. Yaroslavov, N. S. Zefirov, *Tetrahedron* **2014**, *70*, 1408 – 1411.
[17] J. Lou, A. J. Carr, A. J. Watson, S. I. Mattern-Schain, M. D. Best, *Chem. Eur. J.* **2018**, *24*, 3599 – 3607.
[18] J. Takeuchi, A. Ohkubo, H. Yuasa, *Chem. Asian J.* **2015**, *10*, 586 – 594.
[19] T. Holmstrøm, C. M. Pedersen, *J. Org. Chem.* **2019**, *84*, 13242 – 13251.
[20] A. Français, D. Urban, J.-M. Beau, *Angew. Chem. Int. Ed.* **2007**, *46*, 8662 – 8665; *Angew. Chem.* **2007**, *119*, 8816 – 8819.
[21] G. Anderegg, V. Gramlich, *Helv. Chim. Acta* **1994**, *77*, 685 – 690.
[22] C. Lau, R. Bitton, H. Bianco-Peled, D. G. Schultz, D. J. Cookson, S. T. Grosser, J. W. Schneider, *J. Phys. Chem. B* **2006**, *110*, 9027 – 9033.
[23] S. S.-R. Bohr, C. Thorlaksen, R. M. Kühnel, T. Günther-Pomorski, N. S. Hatzakis, *Langmuir* **2020**, *36*, 6473 – 6481.
[24] S. Stella, P. Mesa, J. Thomsen, B. Paul, P. Alcón, S. B. Jensen, B. Saligram, M. E. Moses, N. S. Hatzakis, G. Montoya, *Cell* **2018**, *175*, 1856 – 1871.
[25] R. P. Thomsen, M. G. Malle, A. H. Okholm, S. Krishnan, S. S.-R. Bohr, R. S. Sørensen, O. Ries, S. Vogel, F. C. Simmel, N. S. Hatzakis, J. Kjems, *Nat. Commun.* **2019**, *10*, 5655.
[26] S. S.-R. Bohr, P. M. Lund, A. S. Kallenbach, H. Pinholt, J. Thomsen, L. Iversen, A. Svendsen, S. M. Christensen, N. S. Hatzakis, *Sci. Rep.* **2019**, *9*, 16169.
[27] J. Larsen, N. S. Hatzakis, D. Stamou, *J. Am. Chem. Soc.* **2011**, *133*, 10685 – 10687.

Manuscript received: December 15, 2020
Accepted manuscript online: January 7, 2021
Version of record online: February 22, 2021

 